Assessment of the radiation mode method for *in situ* measurements of loudspeaker systems

Maryna Sanalatii[1,2,3], Lucas Vindrola[2], Clément Vasseur[2], Philippe Herzog[1], Manuel Melon[2], Régine Guillermin[1], Nicolas Poulain[3], and Jean-Christophe Le Roux[3]

[1]*Laboratoire de Mécanique et d'Acoustique (LMA), UPR CNRS 7051, 4 impasse Nikola TESLA, CS 40006, 13000 Marseille, France*
[2]*Laboratoire d'Acoustique de l'Université du Maine (LAUM), UMR CNRS 6613, Av. Olivier Messiaen, 72085 Le Mans cedex 9, France*
[3]*Centre de Transfert de Technologie du Mans (CTTM), 20 rue Thalès de Milet, 72000 Le Mans, France*

Correspondence should be addressed to Manuel Melon (`manuel.melon@univ-lemans.fr`)

ABSTRACT

In this paper, the radiation mode method is used to measure the frequency response and the directivity pattern of loudspeaker systems. This method, which has been successfully applied to speaker measurement in free field conditions, is now tested in a large non-anechoic hall. Two closed box systems and a switchable bi-directive/cardioid subwoofer have been used. Each system is measured first in an anechoic chamber and then in the large hall. The radiation method is then applied to the two different measurement data sets. Results show a good agreement between both conditions. Finally, the influence of the mesh coarsening is studied.

1 Introduction

The measurement of the frequency response and of the directivity characteristics of loudspeaker systems requires free field conditions [1] that can be difficult to achieve for a loudspeaker manufacturer. For instance, large anechoic chambers are very expensive and bad weather conditions can prevent outdoor measurements. For these reasons, many other approaches have been developed to allow measurements in non-anechoic space. Among these, gating of the impulse response can be used to remove wall reflections [2]. Holography based methods have also been proposed to separate the field radiated by the tested source from the field reflected off the room boundaries [3, 4, 5].

The "radiation mode" method has recently been applied to the measurements of loudspeaker systems in free field conditions [6]. This method is based on the numerical computation of the independent radiation solutions (usually named "radiation modes" - acronym "RM") of the tested source. The weights of the modes are experimentally determined using pressure measurements in the vicinity of the source. Typically, about 40 points measured at 30 cm from the source can be sufficient for a bookshelf speaker system. Results reported in [6] showed a good agreement between RM results and direct measurement in an anechoic room.

The next step consists in testing the RM method in non-anechoic conditions. As measurements are performed in the vicinity of the source, one may expect the reverberated field to be marginal compared to the direct sound radiated by the device under test.
In this paper, three speaker systems are tested in a large non-anechoic hall using the RM method. The obtained results are compared with the ones measured in an anechoic chamber. First, the principle of the radiation method is summarized. Then, the tested systems and the measurement room are described. Finally, results are presented and discussed, followed by a discussion about the mesh coarsening.

2 Radiation mode method

The "radiation modes" method is inspired by an inverse acoustic imaging technique: the IBEM-NAH regularized by SVD that has been proposed by Veronesi and Maynard [7]. It has been adapted to the measurement of the vibration patterns of large transformers [8] before being applied to loudspeaker systems [6]. As the derivation of the method has already been described in [6], only a brief summary will be given here.

2.1 Radiation mode computation

The "radiation modes" are computed by solving the Helmholtz integral equation for exterior problem on the surface of the tested speaker system. As no closed form solution exists for arbitrary geometry, the problem is solved numerically by discretizing the source with an adequate mesh to compute its acoustic impedance matrix. Generally, this kind of approach requires a large number of modes to converge towards an accurate solution. As the radiation modes will only be used to calculate the acoustic pressure in the far-field of the source, an interesting simplification can be done by keeping only the real part of the impedance; the imaginary part representing the evanescent contribution is assumed to be negligible at large distances [9].

By using this approach, a smaller number of modes, typically less than 30, are required, thus reducing the computation time. The real part of the impedance matrix is then factorized using a singular value decomposition (SVD), yielding to the determination of the pressure, mode efficiency and volume velocity matrices. The calculation of the radiation modes is performed using a custom BEM code ("FELIN" for "Field ELement INdependence"), developed at LMA, which is dedicated to such field expansion.

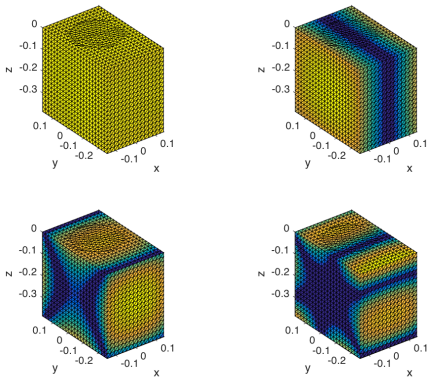

Fig. 1: Visualization of the first (upper left), third (upper right), fifth (lower left) and tenth (lower right) radiation mode at 196 Hz.

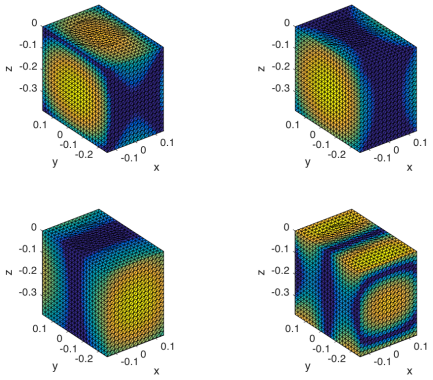

Fig. 2: Visualization of the first (upper left), third (upper right), fifth (lower left) and tenth (lower right) radiation mode at 549 Hz.

Figure 1 depicts four lower order modes (first, third, fifth and tenth modes - sorted by decreasing efficiency) of a bookshelf enclosure at 196 Hz. One can notice that these modes do not particularly fit the geometry of the membrane (shown by a black circle on the upper face). Figure 2 highlights the modification of the mode shapes for a higher frequency (549 Hz). In particular, the first mode is no longer radiating a

monopolar pattern. Please note that, at this frequency, the wavelength is of the same order of magnitude than the largest dimension of the enclosure. Although the mode shapes are depending on frequency, their evolution is slow. This allows to use the “nesting property" which consists in computing expansion coefficients at several frequencies from a RM series computed at a single (higher) frequency [6]. This reduces significantly the RM calculation time for wide-band characterization.

2.2 Mode weighting

Expansion over the RM requires to determine their “weights”, *i.e.* a set of complex valued coefficients (one for each mode), leading to the best approximation of the radiated field. A basic assumption of the method is that the RM weights, determined from pressure measurements at relatively short distances, are valid at any larger distance.

The weights are therefore computed through an inverse method using the transfer matrix linking the pressure measured at identification locations around the source to the RM patterns over the source surface. In addition to the “radiation mode” computation, the FELIN code is thus used to calculate transfer matrices from the RM patterns on the source surface to points located in free space. Two sets of point are defined:

- The identification points: this set defines the positions of the measurement points that allow to determine the weight for each mode. These points are located in the vicinity of the source: 6 to 15 points per source surface are chosen at 20 or 30 cm of each wall.
- The computation points: this set gives the locations of the target points for which the response of the tested speaker is needed, *i.e.* on-axis, polar or 3D directivity positions.

The choice of the locations of the identification points result from a trade-off between achieving far-field conditions and keeping a good signal-to-noise ratio. A distance close to the size of the source is usually adequate, although a somewhat shorter one might be used [9]. This allows to perform measurement *in situ*, provided that direct field dominates at the identification points.
The number of modes required to describe the complexity of the source radiation increases with frequency. The modal series may be truncated to the most significant RM’s, thus reducing the number of measurements required for the identification. In this paper we only keep the most efficient terms, their number being chosen so that they represents 98% of the accumulated efficiency. Their number may thus be determined during the computation and does not depend on measurements as long as the number of identification points is larger than the number of modes to build an over-determined system [8].

2.3 Radiated pressure calculation

The weights previously computed are then applied to the matrix that links the calculation points to the RM, in order to compute the pressure response at the desired locations.
A flow chart summarizing the steps required by the RM method is shown in Fig. 3. Note that the computation phase needs to be performed only once for a given box shape, allowing then to process measurements for several configurations (different loudspeakers models and locations, filters, etc).

3 Measurements

3.1 Tested systems

Three systems have been used: two closed box systems and a subwoofer with two directivity presets. The two closed box systems are the ones described in [6]:

- The first one, denoted SC1 (for "Single Closed box 1"), is a bookshelf system with outer dimensions of 42 cm$\times$24 cm$\times$34 cm) equipped with a Monacor SPH-8M-8 loudspeaker featuring a 17.5 cm $\varnothing$ membrane;
- The second one, denoted SC2 (for “Single Closed box 2”), is a column system with outer dimensions of 19 cm$\times$75 cm$\times$16 cm equipped with a Fostex FE126En loudspeaker featuring a 9 cm $\varnothing$ membrane.

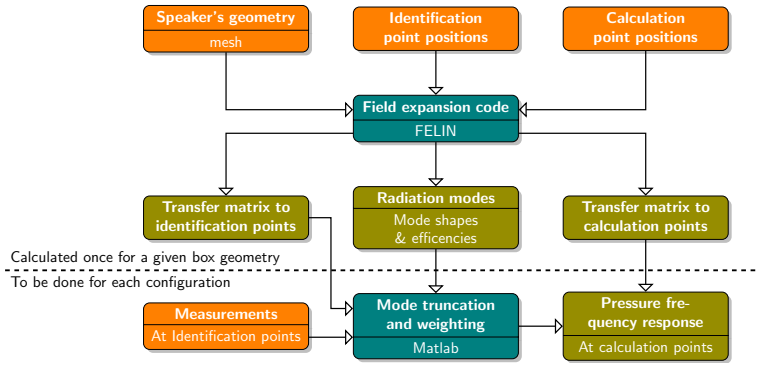

Fig. 3: RM method flow chart, input data in orange and output data in olive color.

The third system is made of two identical bass reflex enclosures (39.4 cm×44.4 cm ×34.4 cm) tied together giving a largest dimension of $39.4 \times 2 = 79.2$ cm (see Fig. 4). One Visaton WS-17E-4 Ohm is mounted on each reflex enclosure. An active filter has been designed to obtain a cardioid pattern using an approach proposed by Boone [10]. This preset will be referred below as CDR for "Cardioid Dual Reflex". Another radiation condition can be achieved by removing the filter and inverting the polarity of one of the two speakers to get a figure-of-eight pattern. This preset is denoted BDR for "Bi-directive Dual Reflex".

3.2 Speaker system meshes

All tested systems have been discretized with triangular elements. The actual membrane shape has not been taken into account : it is considered as a planar disc included into the supporting face of the box. The maximum element size for each system is given in Table 1. Please note that for SC1 and SC2 systems, different mesh sizes have been used, one for the enclosure and the other for the membrane. Table 1 also gives the maximum computing frequencies according to a "10 elements per wavelength" criterion, the total number of elements per system, the computing time and the number of identification points that has been used for the experiments.

3.3 Measurement rooms

In situ measurements have been performed in a large hall of the university in Le Mans. The outer walls dimensions are approximately 9 m×20.5 m×14 m

System	SC1	SC2	DR
Box mesh size Max. frequency	2 cm 1700 Hz	10 cm 340 Hz	5 cm 680 Hz
Piston mesh size Max. frequency	5 mm 6800 Hz	1 cm 3400 Hz	5 cm 680 Hz
Total number of elements	5364	520	1298
RM computing time	10 h for 37 freq.	$2'41''$ for 37 freq.	$38'58''$ for 171 freq.
Number of identification points	37	39	58

Table 1: Mesh characteristics for the different systems.

Fig. 4: Picture of the third system (BDR/CDR) in the large hall.

(see Fig. 5). The tested source is mounted on a stand 2 m above the ground (nearest reflective surface). The reverberation time gently decreases from 2.3 s in the 125 Hz octave band to 0.9 s in the 4000 Hz octave band. From these data, the critical distances[1] can be computed: $\simeq$ 1.9 m (125 Hz) and $\simeq$ 3.3 m (4000 Hz). These values are much larger than the measuring distances (20 or 30 cm), ensuring the predominance of the direct field in pressure measurements. The positions of the identification points for the SC1 system is shown on Fig. 6.

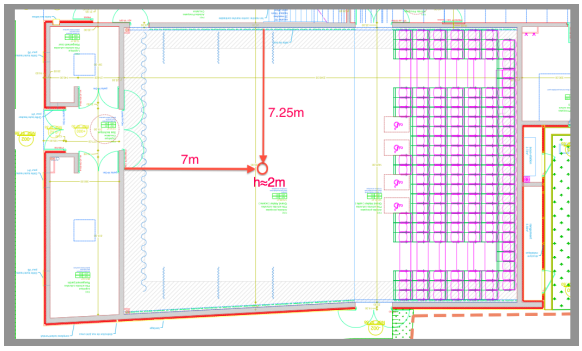

Fig. 5: Large hall plan: the circle shows the position of the tested speaker. Distances to the nearest surfaces are also indicated.

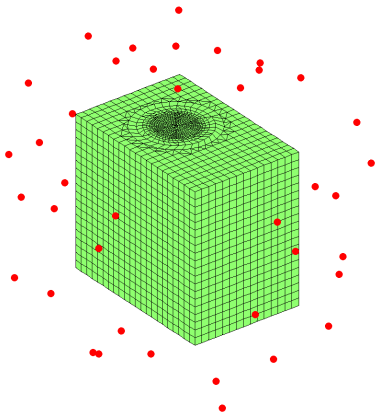

Fig. 6: Positions of the 37 identification points used for the SC1 system.

Anechoic measurements were performed in the LAUM anechoic room (4.9 m$\times$3.9 m$\times$3.6 m between wedge tips) with a cut-off frequency around 100 Hz.

3.4 Measurement procedure

For all experiments, each system was driven by a band limited white noise signal. Pressure signals were recorded by moving the same microphone along all locations, thus avoiding any calibration issues. Frequency responses, giving the ratio of the measured pressure over the input voltage, were computed using 200 averages. When the dimensions of the anechoic chamber allowed it, a “classic" measurement of the frequency response or directivity curve has been performed and is used as a reference. Therefore, all the curves denoted below as "reference" will correspond to direct pressure measurements in anechoic conditions. Magenta vertical lines are also drawn when required to indicate the maximum frequency allowed for RM computation, according to table 1.

4 Results

4.1 On-axis response

The RM method has been first applied to the SC1 and SC2 closed box systems. For these two configurations, 37 (resp. 39) identification points, located at 20 cm (resp. 30 cm) from the sources, have been used. The on-axis pressure is plotted on Fig. 7 for SC1 and on Fig. 8 for SC2. The results obtained by the RM method computed from measurements close to the box in anechoic conditions agree very well to the reference values for both systems. For the RM method computed with the *in situ* data, the results are also very good. There is, however, a slight underestimation of the on-axis level for SC1 above 3 kHz.

One might be surprised that better *in situ* results are obtained at higher frequencies for SC2, rather than for SC1 despite its more detailed mesh (5364 vs 520 elements). The reason may be due to the smallest membrane diameter (9 cm) of SC2 which exhibit a less directive pattern than SC1 (17.5 cm $\varnothing$). The identification measurements at the back of SC1 may then have resulted into a lower SNR. This effect is less prejudicial for anechoic measurements.

[1] Distance at which the SPL of the direct sound is equal to the SPL of the reverberant sound

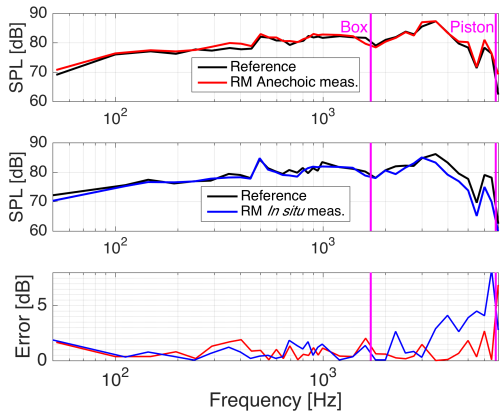

Fig. 7: On-axis sound pressure level for SC1. Upper graph: anechoic room - black: reference, red: RM method. Middle graph: *in situ* conditions - black: reference, blue: RM method. Lower graph: error in dB between the reference and the RM method data - red: anechoic, blue: *in situ*

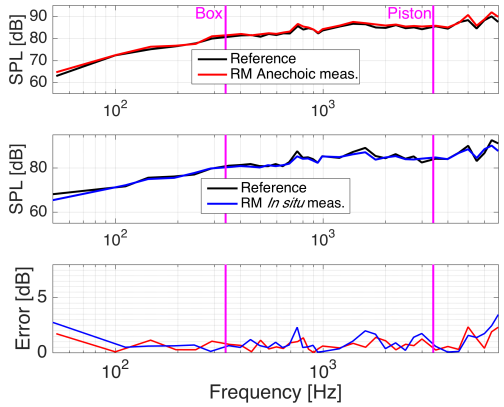

Fig. 8: On-axis sound pressure leval for SC2. Upper graph: anechoic room - black: reference, red: RM method. Middle graph: *in situ* conditions - black: reference, blue: RM method. Lower graph: error in dB between the reference and the RM method data - red: anechoic, blue: *in situ*

Results obtained for the BDR/CDR systems with 58 identification points are plotted on Fig. 9. For the two directivity presets, the agreement between the different methods is fairly good: *in situ* results are very close to the free field ones. Larger discrepancy peaks are also observed above 500 Hz for the CDR system. These errors might come from a lower signal to noise ratio in this frequency range for which the system has a lower efficiency.

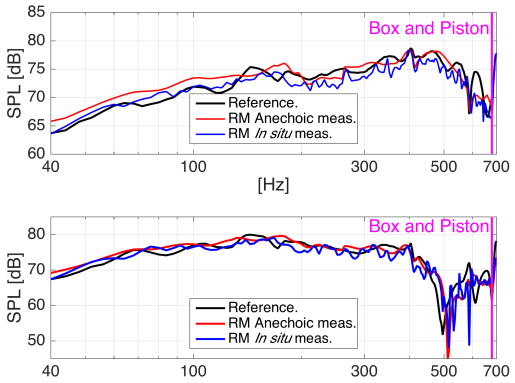

Fig. 9: On-axis sound pressure level for the dual reflex system (upper graph: BDR, lower graph: CDR). Black: reference, red: RM method (anechoic room), blue: RM method (*in situ*).

4.2 Directivity

The estimation of the on-axis level by the RM method in a large hall gave reliable results for on-axis response. The next step consists in assessing the method for other angles. The directivity pattern of loudspeaker systems is a far-field quantity that should therefore only be measured at a large distance from the source, typically greater than the source largest dimension and/or larger than the minimum wavelength. This distance might become larger than 4 m for large sound reinforcement systems, especially line arrays (very tall devices) or for subwoofers (generating very low frequencies). In such cases, anechoic chambers can barely be used because of their restricted working volume leading to unreliable measurements at large distances from the source.

Since the work of Weinreich and Arnold [11], several methods based on near-field measurements

coupled to extrapolation to the far-field using a set of mathematical functions have been developed. These approaches generally involve spherical [12, 13, 14] or cylindrical [5] harmonic expansions. However, a very dense mesurement grid is needed to fulfill the Nyquist spatial sampling rate when looking for high accuracy directivity pattern. For instance, a full sphere recording, with a 5° angle grid, requires 2522 unique points (or 64442 unique points at 1° resolution). These very large numbers show the difficulty to obtain a reliable radiation pattern, especially at high frequencies for which the 5° resolution may be insufficient. To overcome this drawback, several solutions have been proposed involving extrapolation of the missing data [15], the HELS Method [16] or the use of symmetries in the tested source radiation pattern [5].

For the RM method, the possibility to use a sparse sampling results from two main properties:

- Unlike spherical harmonics functions that are generic functions, the RM are specific to the geometry of the tested source, and are thus well adapted to its radiation characterization.
- The use of the real part of the impedance while discarding the imaginary terms also allows to reduce the number of measurement positions required by the inverse problem.

The RM method is now applied to the measurement of directivity pattern of the dual bass-reflex source. Figure 10 plots the sound pressure levels at 1 m for the CDR configuration as a function of the angle for 3 different methods: the reference one and the RM method in anechoic and *in situ* conditions. The three curves agree well although some discrepancies may be observed around angles with local minima.

One interesting feature of the RM method is that it allows to compute directivity patterns at large distances although they might not be measurable in practice. In our case, the working volume of the anechoic chamber does not allow measurements at 4 m distance, even more with the source at the room's center. Figure 11 and 12 respectively plot the directivity pattern of BDR and CDR systems estimated at 4 m. One can see that extrapolations from data measured in the anechoic room or in the large hall are very close to each other for both

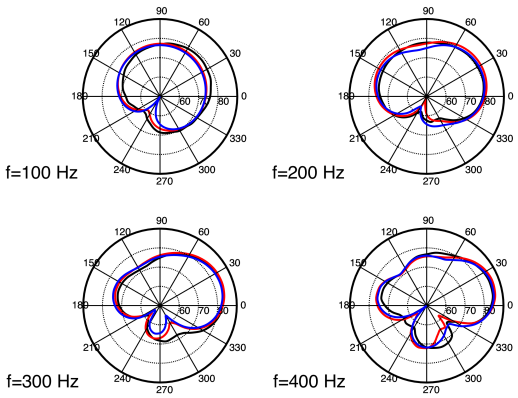

Fig. 10: Comparison of SPL versus angle at 1 m for the CDR system: reference (black) or computation with the RM method from anechoic (blue) or *in situ* (red) data.

systems. Although no reference data are available at these distances, the estimated RM directivities agree well with the expected shapes: figure-of-eight for BDR and cardioid for CDR, as long as the wavelength is large compared to the source size ($\simeq$ up to $200Hz$).

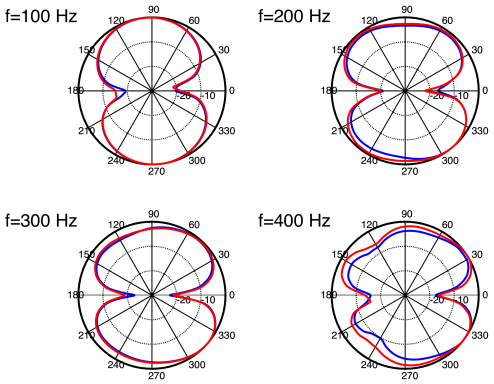

Fig. 11: Directivity patterns for BDR at 4 m computed with the RM method from anechoic (blue) or *in situ* (red) data

4.3 Mesh coarsening

One important aspect of the RM method concerns the refinement of the mesh: should all the geometrical details of the membrane be discretized? What is

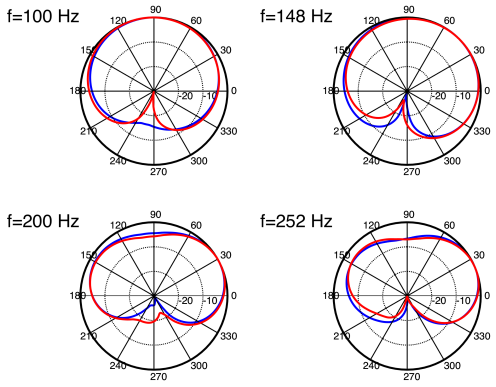

Fig. 12: Directivity patterns for CDR at 4 m computed with the RM method from anechoic (blue) or *in situ* (red) data

the optimal element size? To explore this point, the RM have been computed for 4 meshes (see Table 2). Among the proposed discretizations, mesh A describes the real profile of the membrane while mesh B to mesh D approximate it with a planar piston. Meshes B and C have a refined mesh for the membrane and a loose one for the enclosure. Mesh D has the same element size for both enclosure and membrane.

Figure 13 plots the on-axis SPL at 1 m (measurement data and RM results for the 4 meshes with 42 identification points). The agreement between the different curves is very good except for mesh D that has a uniform mesh size of 2 cm. Surprisingly, mesh C, that has a rough mesh of the enclosure (10 cm) and the same membrane element size (2 cm) as mesh D gives a very good estimate of the on-axis pressure. This can be explained by the fact that the mesh contrast gives a larger importance to the membrane, which might be favorable for the on-axis frequency response.

Figure 14 gives the SPL at (1 m, 90°) for the same meshes. At this position, the importance of the box discretization is emphasized, especially at higher frequencies where the speaker is more directive. In this case, meshes A to C gives good results up to 2 kHz. Above this frequency, only meshes A & B give acceptable results (with some error peaks). The lower performances of mesh C might then be due to the larger enclosure mesh size.

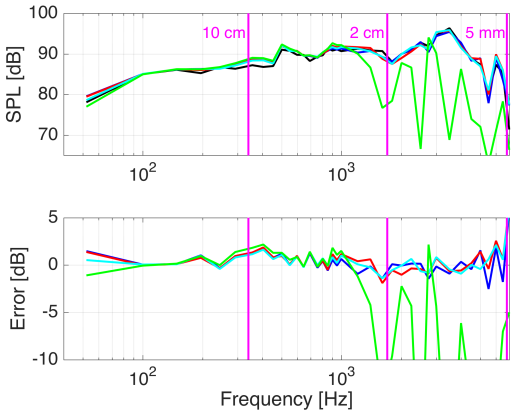

Fig. 13: Influence of the mesh corsening for on-axis response. Upper graph: SPL at 1 m for 1 V. Black: reference, blue: mesh A, red mesh B, cyan mesh C, green: mesh D. Lower graph: error in dB between the direct measurement and the RM results.

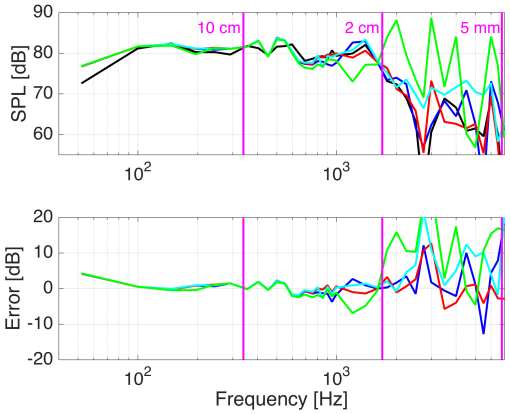

Fig. 14: Influence of the mesh corsening at 90°. Upper graph: SPL at 1m for 1 V. Black: reference, blue: mesh A, red mesh B, cyan mesh C, green: mesh D. Lower graph: error in dB between the direct measurement and the RM results.

Mesh	A	B	C	D
Membrane geometry	Real profile	Piston	Piston	Piston
Box mesh size	2 cm	2 cm	10 cm	2 cm
Membrane mesh size	5 mm	5 mm	2 cm	2 cm
RM computing time	33.2 h	10 h	$3' 8''$	8.16 h

Table 2: Mesh sizes of the bookshelf enclosure (SC1) used in section 4.3

To conclude this section, the following rule of thumbs concerning the mesh design could be used:

- A finer mesh should be used over zones where the vibration or its variation is expected to be large (membrane, around suspension, vent, etc);
- The box may be discretized with a looser mesh, at the price of less accurate off-axis results.

5 Discussion

In this paper, the RM method has been tested in a large hall of the university, a non-anechoic environment which however ensures that the reverberated pressure near the tested source can be expected to be marginal compared to the direct field. Results obtained *in situ* were found to be very close to the one obtained in an anechoic room, for both on-axis response and directivity patterns, thus confirming the above assumption. This outcome opens the way for the use of RM method in normal rooms. Future work will have to investigate whether smaller rooms with reasonable damping allow to reach a similar accuracy.

The RM method also allowed to measure the directivity patterns of a dual reflex enclosure with cardioid and bi-directive presets with only 58 measurement points located at 30 cm from of the source. Although not ideal, the RM approach can thus be considered as an interesting trade-off between accuracy and experimental cost.

The quality of the mesh size has also been investigated giving some hints for an appropriate discretization of the tested system. One remaining question concerns the choice of the number and positions of the identification points in the vicinity of the source. In this paper, an almost even coverage of the system has been chosen and yielded good results. However, an automated procedure that would give the optimal set of identification points would be of great help. We are therefore seeking for a method that would automatically pick out inliers (positions that bring much information) and reject outliers (positions that are very sensitive to noise).

References

[1] IEC 60268-5, "Sound system equipment - Part 5: Loudspeakers," *Standard of the International Electrotechnical Commission*, 2007.

[2] Berman, J. and Fincham, L., "The Application of Digital Techniques to the Measurement of Loudspeakers," *J. Audio Eng. Soc.*, 25(6), pp. 370–384, 1977.

[3] Melon, M., Langrenne, C., Rousseau, D., and Herzog, P., "Comparison of Four Subwoofer Measurement Techniques," *J. Audio Eng. Soc.*, 55(12), pp. 1077–1091, 2007.

[4] Melon, M., Langrenne, C., and Herzog, P., "Evaluation of a method for the measurement of subwoofers in usual rooms," *J. Acoust. Soc. Am.*, 127(1), pp. 256–263, 2010.

[5] Klippel, W. and Bellmann, C., "Holographic Nearfield Measurement of Loudspeaker Directivity," in *the 141th AES Convention*, preprint 9598, Los Angeles, USA, 2016 September 29th - October 1st.

[6] Sanalatii, M., Herzog, P., Melon, M., Guillermin, R., Le Roux, J.-C., and Poulain, N., "Measurement of the frequency and angular responses of loudspeaker systems using radiation modes," in *the 141th AES Convention*, preprint 9615, Los Angeles, USA, 2016 September 29th - October 1st.

[7] Veronesi, W. and Maynard, J., "Digital holographic reconstruction of sources with arbitrary

shaped surfaces," *J. Acoust. Soc. Am.*, 85(2), pp. 588–598, 1989.

[8] Herzog, P., Guillermin, R., Lorin, P., and Chritin, V., "Identification of a vibration pattern from pressure measurements and radiation modes," in *EuroNoise*, Maastricht (NL), 2015.

[9] Herzog, P. and Schevin, O., "Estimation du degré de complexité d'un modèle de source vibrante," in *Actes du 6ème Congrès Français d'Acoustique*, 075, Lille, FR, 2002.

[10] Boone, M. M. and Ouweltjes, O., "Design of a Loudspeaker System with a Low-Frequency Cardiodlike Radiation Pattern," *J. Audio Eng. Soc*, 45(9), pp. 702–707, 1997.

[11] Weinreich, G. and Arnold, E. B., "Method for measuring acoustic radiation fields," *The Journal of the Acoustical Society of America*, 68(2), pp. 404–411, 1980, doi:10.1121/1.384751.

[12] Angus, J. A. S. and Evans, M. J., "Polar Pattern Measurement and Representation with Surface Spherical Harmonics," in *Audio Engineering Society Convention 124*, preprint 4717, Amsterdam, NL, 1998.

[13] Fazi, F., Brunel, V., Nelson, P.-A., Hörchens, L., and Seo, J., "Measurement and Fourier-Bessel Analysis of Loudspeakers Radiation Patterns Using a Spherical Array of Microphones." in *Audio Engineering Society Convention 124*, preprint 7354, Amsterdam, NL, 2008.

[14] Melon, M., Langrenne, C., Thomas, O., and Garcia, A., "Comparison between Measurement and Boundary Element Modelization of Subwoofers," in *Audio Engineering Society Convention 127*, preprint 7845, New York, USA, 2009.

[15] Panzer, J. and Ponteggia, D., "Inverse Distance Weighting for Extrapolating Balloon-Directivity-Plots," in *Audio Engineering Society Convention 131*, preprint 8473, New York, USA, 2011.

[16] Keele, D. B. D., Jr., Lu, H., and Wu, S., "High-Accuracy Full-Sphere Electro Acoustic Polar Measurements at High Frequencies using the HELS Method," in *Audio Engineering Society Convention 121*, preprint 6881, San Francisco, USA, 2006.